Stress Relaxation Behavior of Unidirectional Carbon/Epoxy Composites at Elevated Temperature and Analysis Using Viscoplasticity Model*

Masamichi KAWAI**, Takeshi KAZAMA**, Yoichi MASUKO**, Hiroshi TSUDA***, Jun TAKAHASHI**** and Kiyoshi KEMMOCHI†

Off-axis stress relaxation behavior of unidirectional T800H/3631 carbon/epoxy composite exposed to high temperature is examined at relatively high tensile strain levels, and a phenomenological viscoplasticity model is tested on the capability to describe the time-dependent response observed. First, stress relaxation tests are performed at 100°C on plain coupon specimens with different fiber orientations, $\theta=0$, 10, 30, 45, and 90°. For each of the fiber orientations, in principle, stress relaxation tests are carried out at three different strain levels. The relaxation of axial stress in the unidirectional composite is clearly observed, regardless of the fiber orientation. Just after the total strain hold, the axial stress quickly relaxes with time in a short period. The stress relaxation rate of the composite tends to become zero, irrespective of the fiber orientation. The associated relaxation modulus depends on the level of strain. The entire process of the prior instantaneous tensile response and the subsequent off-axis stress relaxation behavior is simulated using a macromechanical viscoplasticity model based on an overstress concept. It is demonstrated that the model succeeds in adequately reproducing the off-axis stress relaxation behavior of the unidirectional composite laminate.

Key Words: Polymer Matrix Composites, Unidirectional Composites, Time-Dependent Behavior, Stress Relaxation, Off-Axis Specimens, Viscoplasticity, Macromechanics Model, Carbon Fiber, Epoxy, High Temperature

1. Introduction

Glassy polymers have a strong tendency of time-dependent deformation and fracture[1]-[3]. Since the long molecular chains of glassy polymers change with time to a more stable configuration at a given temperature, their mechanical properties vary with time under stress-free conditions[4],[5]. These imply that the deformation and fracture behaviors of polymer matrix composites (PMCs) subjected to off-axis loading should be significantly influenced by the time-dependent properties of polymer matrices. Regarding the high-temperature durability of PMC laminates for advanced aerospace structures, the matrix-dominated responses to shear loading are crucial. To evaluate the performance and reliability of PMCs, therefore, it is very important to accumulate fundamental data on the time-dependent behavior under various loading and temperature conditions. To establish a rational design procedure based on the local analysis of PMC structures, it is also prerequisite to develop a constitutive model that can describe the time-dependent behavior of PMCs.

Observation and modeling of the time-dependent behavior of PMCs have been attempted, for example,

* Received 30th May, 2003 (No. 02-0193). Japanese Original: Trans. Jpn. Soc. Mech. Eng., Vol. 68, No. 673, A (2002), pp. 1320-1327 (Received 21st February, 2002)

** Institute of Engineering Mechanics and Systems, University of Tsukuba, 1-1-1 Tennodai, Tsukuba 305-8573, Japan. E-mail: mkawai@kz.tsukuba.ac.jp

*** Smart Structure Research Center, AIST, 1-1-1 Higashi, Tsukuba 305-8562, Japan

**** Department of Environmental and Ocean Engineering, University of Tokyo, 7-3-1 Hongo, Bunkyo-ku, Tokyo 113-8656, Japan

† Functional Machinery and Mechanics, Shinshu University, 3-15-1 Tokida, Ueda 386-8567, Japan

by the following researchers. Beckwith[6] observed the creep and creep strain recovery behavior of unidirectional and angle-ply laminates of glass-fiber-reinforced composites (GFRPs), and applied the linear viscoelasticity theory to the creep behavior of those laminates. Sullivan[7] examined the off-axis creep behavior of unidirectional GFRP laminates at relatively low stress levels. It was also shown[7] that the Boltzmann superposition principle was well applied to the short-term creep behavior, and the effective time theory[8] was suitable for the long-term behavior. Similar results are reported for carbon fiber-reinforced composites (CFRPs). Tuttle and Brinson[9] examined the creep and creep strain recovery behavior of the unidirectional and symmetric laminates of T300/5208, and successfully applied the classical laminated plate theory and a nonlinear viscoelasticity model[10] for individual plies to the description of the creep behavior observed. Katouzian et al.[11] investigated the creep behavior of [90] and [±45] laminates made of unidirectional T800/Epoxy and AS4/PEEK systems at various temperatures and stress levels, and showed that the creep behavior was appropriately described by a nonlinear viscoelasticity model[10].

Viscoelasticity models are favored for the description of the time-dependent behavior of PMCs. For cases of relatively low stress or strain, the time-dependent behavior of PMCs is characterized by linear and nonlinear viscoelastic responses of polymer matrices, as demonstrated in the above reports. When relatively high stresses or strains are applied, however, the time-dependent behavior of glassy polymers tends to deviate from the predictions using viscoelasticity models. This is partly because loading of solid polymers to high stress or strain levels results in time-dependent inelastic deformation[4]. To consider the effects of the time-dependent inelastic response of PMCs to relatively high stress or strain, Tuttle et al.[12] added a viscoplastic strain term to the Schapery nonlinear viscoelasticity model and successfully applied the viscoelastic-viscoplastic model to the creep behavior of the [90] and [±45] laminates of the IM7/5260 system. In place of the nonlinear integral representations modified as above, the constitutive models in differential forms may also be applied to the time-dependent behavior of PMCs. Ha and Springer[13] developed a rate form of the constitutive model for unidirectional composites on the basis of the viscoplasticity model for isotropic materials[14]. Similar viscoplasticity models were proposed by Gates and Sun[15] and Wang et al.[16],[17] Chung et al.[18] also developed a creep model for unidirectional laminates on the basis of the Blackburn creep equation for isotropic materials. It has been demonstrated that those viscoplasticity models in differential forms succeed in adequately describing the time- and rate-dependent behavior for various kinds of PMCs. However, systematic data for basic creep behavior of unidirectional PMC laminates at high temperature over a wide range of stress are limited. Very few studies have been reported on the stress relaxation effect in unidirectional PMC laminates. To confirm the validity of the rate form of the viscoplasticity model for the time-dependent behavior of unidirectional PMC laminates at relatively high stress/strain levels and high temperatures, therefore, further studies for evaluation is needed.

In the present study, characteristics of the high-temperature off-axis stress relaxation behavior of a unidirectional CFRP laminate at relatively high strain levels are first examined. To observe the effects of fiber orientation and magnitude of sustained strain, stress relaxation tests are performed at three different strain levels on five kinds of unnotched coupon specimens with different fiber orientations. The off-axis time-dependent behavior is also explored by repeated loading-unloading experiments with gradual increase of the peak stress level in tension. Then, the validity of a phenomenological viscoplasticity model for the off-axis stress relaxation behavior is evaluated on the basis of the experimental results obtained.

2. Experiments

2.1 Materials and specimens

The material used in this study was a unidirectional fiber-reinforced composite laminate fabricated from prepreg tape (P2212-15, TORAY) that consists of the carbon fiber (T800H) and the thermosetting epoxy resin (#3631). The volume fraction of the fibers was V_f=51.7%, and the lay-up of the laminate was $[0]_{12}$. The glass transition temperature of the epoxy resin is 215°C. The unidirectional T800H/3631 laminate was cured at 180°C for two hours in an autoclave.

Five kinds of plain coupon specimens with different fiber orientations (off-axis angle θ=0, 10, 30, 45, 90°C) were cut from 400 mm by 400 mm unidirectional laminate panels. The shape and dimensions of the off-axis specimens were based on the testing standard JIS K7073[19]; as shown in Fig. 1, the specimen length L was 200 mm and the thickness t was 1.7 mm. The specimen width was 10 mm for θ=0° and 20 mm for other off-axis angles. Rectangular-shaped aluminum-alloy tabs were attached on both ends of the specimens using epoxy adhesive (Araldate); the thickness of the end-tabs was 1.0 mm. The tabs were bonded at 90°C in the oven (Gravity Oven LG-112, ESPEC); the specimens were exposed to that temper-

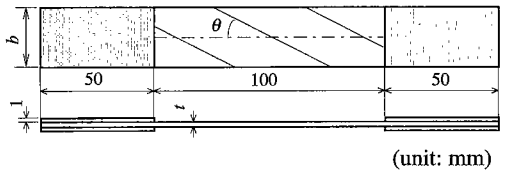

Fig. 1 Specimen geometry (dimensions in mm)

ature for one hour to increase the adhesive strength.

2.2 Test procedure

Off-axis stress relaxation tests were carried out at 100°C at three strain levels for each fiber orientation. The middle strain level corresponded to the stress equal to 60% of the static tensile strength at the test temperature. The duration of the strain hold was specified to be five hours. Off-axis stress relaxation tests were conducted under stroke displacement control. Hence, the nominal strain ε_R over the gauge-length part of specimen was kept constant, but the local strain in the gauge part was not.

To obtain the reference stress-strain curves at 100°C for the specimens, static tension tests were carried out with stroke control at the rate of 1.0 mm/min on the basis of the testing standard JIS K7087[20]. Repeated loading/unloading tension tests were also conducted to elucidate the characteristics of the stress-strain curves. For the stress relaxation tests, the loading to the desired strain was controlled at a constant stroke rate of 1.0 mm/min.

These tests were performed using a closed-loop hydraulic MTS-810 testing machine of the dual servovalve type; the flow capacities of the low- and high-speed servovalves were 4 L/min and 19 L/min, respectively. To raise the temperature of the specimens, a heating chamber with precise digital control capability was employed. The specimens were heated to 100°C in air without applying load, and they were preconditioned in the test environment for 60 minutes prior to the test. The specimens were clamped in the heating chamber by high-temperature hydraulic wedge grips fitted on the testing machine. The deviation from the prescribed specimen temperature was less than 1.0°C. Humidity in the heating chamber was not controlled. Longitudinal and lateral strains of each off-axis specimen were monitored with two-element L-type rosette strain gauges. These strain gauges were mounted back to back at the center of each specimen.

3. Experimental Results

The in-plane specimen coordinate system is denoted as (x, y), and the x-axis is taken in the loading direction. The principal axes of material anisotropy, i.e., the fiber coordinate system, are expressed as (1,2), the 1-axis being in the fiber direction.

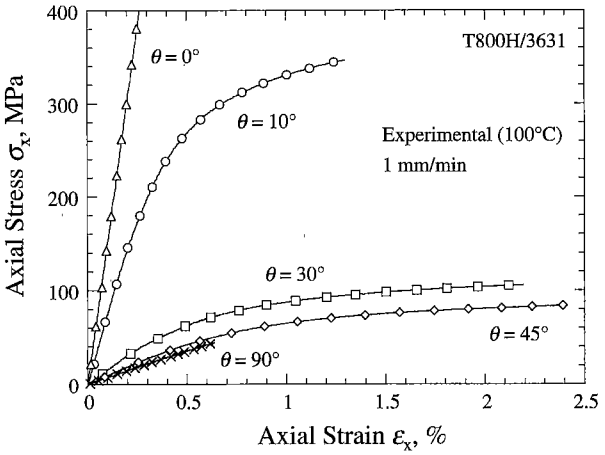

Fig. 2 Tensile stress-strain relationships of unidirectional T800H/3631 at 100°C

3.1 Off-axis static tensile behavior

Tensile stress-strain relationships for various fiber orientations are shown in Fig. 2. A significant nonlinear behavior is observed for the off-axis angles in the range $10° \leq \theta \leq 45°$. As for the fiber and transverse directions ($\theta=0$, 90°), the stress-strain curves are almost linear up to fracture.

It was confirmed that the fiber orientation dependences of the Young's modulus E_x and the Poisson's ratio ν_{xy} were adequately predicted using the orthotropic linear elasticity theory. The off-axis tensile strengths were appropriately described in terms of the Tsai-Hill static failure criterion. The on-axis engineering elastic constants based on the static tension tests are listed in Table 1.

3.2 Successive loading and unloading behavior

The stress - strain responses to repeated loading/unloading tension are shown in Figs. 3(a) - (c) for fiber orientations $\theta=10$, 30, and 45°, respectively. Two important features are revealed for the off-axis nonlinear behavior of the unidirectional T800H/3631 laminate at 100°C. The first feature is that a certain amount of strain remains after complete unloading. The magnitude of residual strain becomes higher with greater prior maximum tensile stress attained just before unloading. The residual strain did not completely recover even after a long time of keeping load at zero. This suggests that the off-axis nonlinear deformation includes an inelastic part. It may be considered that the inelastic contribution to the off-axis deformation is governed by the inelastic property of the epoxy resin employed, since the axial response of off-axis specimens is governed by the shear response of the matrix along fibers. The second feature is that a large stress-strain hysteresis appears

Table 1 Engineering elastic constants for unidirectional T800H/3631 laminates at 100°C

E_1 (GPa)	E_2 (GPa)	G_{12} (GPa)	ν_{12}	ν_{21}
151	7.29	3.51	0.355	0.007

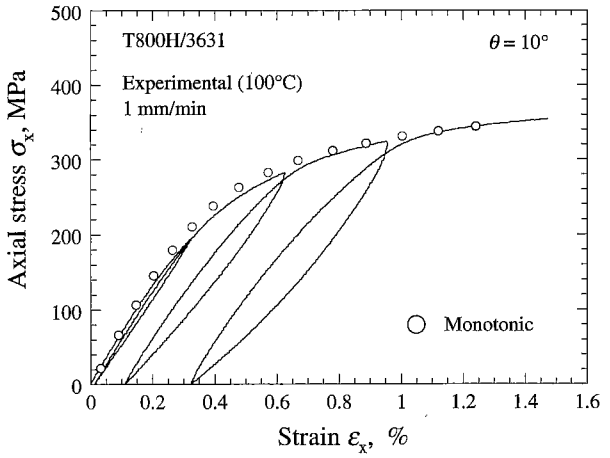

(a) θ=10°

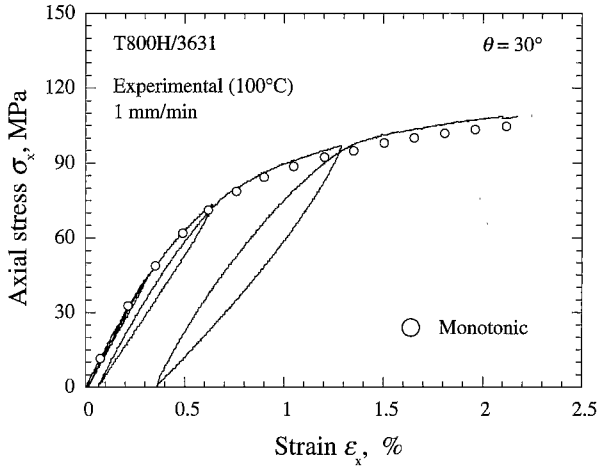

(b) θ=30°

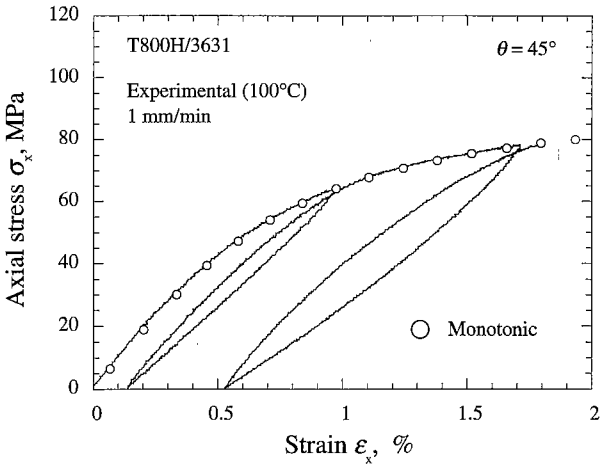

(c) θ=45°

Fig. 3 Off-axis hysteretic responses of unidirectional T800H/3631 at 100°C

upon cyclic loading with a sequence of loading, unloading and reloading. The width of the hysteresis loop becomes larger with increasing peak level of the prior tensile stress. Comparison between the cyclic responses for all fiber orientations showed that the width of the hysteresis loop became more significant for the range θ=10 - 45°.

3.3 Off-axis stress relaxation behavior

Off-axis stress relaxation responses for fiber orientations θ=10, 45, and 90° are shown in Figs. 4(a) - (c), respectively. The stress relaxation data on the 45 and 90° specimens are presented only for two strain levels, because of unexpected rupture during prior loading. The stress relaxation effect is clearly observed in all off-axis specimens. The amount of stress relaxation depends on the total strain kept constant, and it becomes more significant at a higher strain level. Upon holding the strain, the axial stress quickly relaxes and then tends to approach a steady-state value associated with the sustained strain. Namely, the stress relaxation rate decreases to zero in a short period regardless of the strain level and the fiber orientation. On comparing the stress relaxation curves (figures not shown), we see that the stress relaxation takes place more significantly at a higher strain level regardless of the fiber orientation. A few additional tests were conducted under the same conditions, and the results confirmed that the characteristic features of the off-axis stress relaxation shown in Fig. 4 were unchanged by the data scatter.

On inspecting the stress relaxation response for θ=90° in Fig. 4(c), we note that the axial stress increases slightly after a certain amount of normal stress relaxation. Such an anomalous response is also observed for other fiber orientations, although it is less significant. A similar anomaly is observed for the transverse creep behavior of the same type of unidirectional composite[21]. This phenomenon may be ascribed to the volume contraction of the epoxy resin due to physical aging[4] and drying[22].

According to the specifications of the adhesive bonding tabs attached to the specimens, the adhesion is sufficiently high. However, the amount of stress relaxation for the fiber direction (θ=0°) is greater than that predicted using the rule of mixture[23]. This throws suspicion on the result that a certain amount of shear deformation occurred in the adhesive of the tabs during the stress relaxation tests for the fiber direction. It is believed that the stress relaxation data for other fiber orientations are reliable, since the axial stress associated with the hold strain is much lower than that for the fiber direction. In the following discussion, therefore, we limit ourselves to fiber orientations θ>0°, at which the effect of tab slipping is

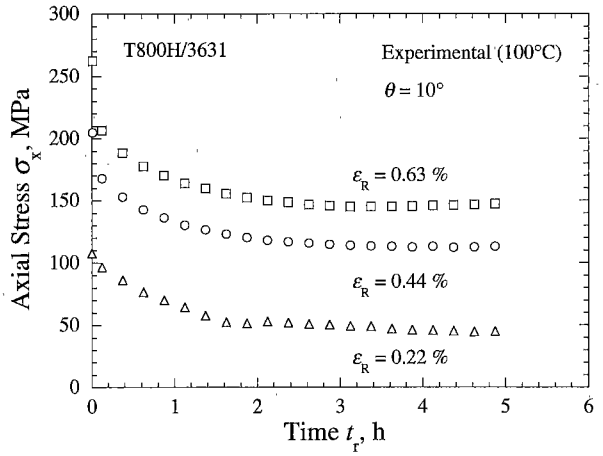

(a) $\theta=10°$

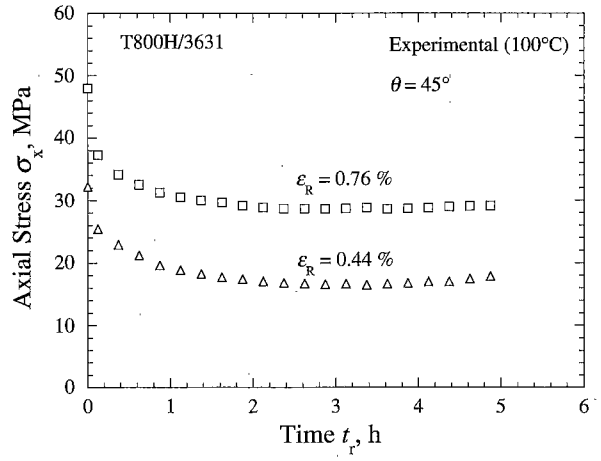

(b) $\theta=30°$

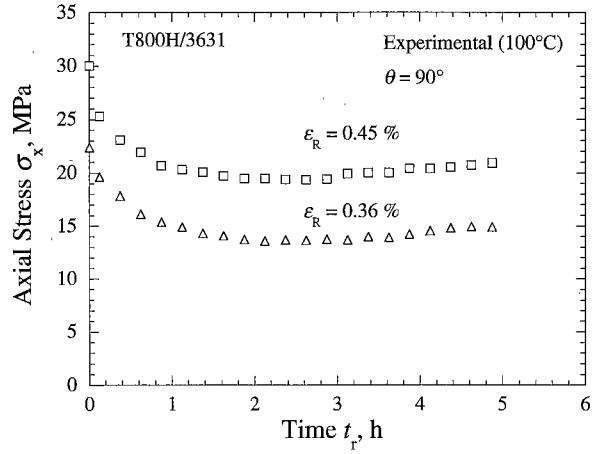

(c) $\theta=90°$

Fig. 4 Off-axis stress relaxation responses of unidirectional T800H/3631 at 100°C

considered to be negligible.

3.4 Off-axis stress relaxation modulus

Figure 5(a) and (b) show plots of the stress relaxation modulus σ_x/ε_R against time t_R on logarithmic scale for the fiber orientations $\theta=10$ and 45°,

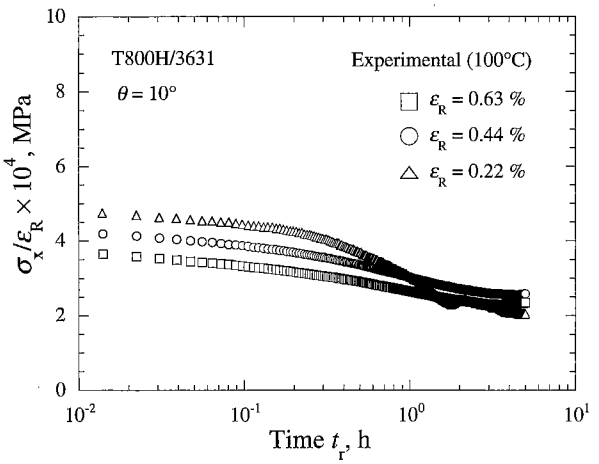

(a) $\theta=10°$

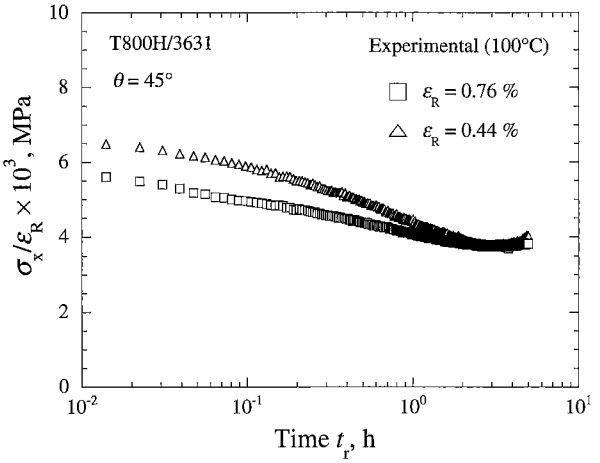

(b) $\theta=45°$

Fig. 5 Relationship between the relaxation modulus and time for unidirectional T800H3631 at 100°C

respectively. From these figures, we can see that the stress relaxation modulus depends on the level of strain sustained. This indicates that the Boltzmann superposition principle[4),(5)] cannot be accurately applied to the off-axis stress relaxation behavior observed.

4. Modeling and Simulation of the Off-Axis Stress Relaxation Behavior

Considering the nonlinear stress-strain response to off-axis loading and the permanent strain after unloading, together with the strain dependence of the relaxation modulus, we inferred that the off-axis stress relaxation behavior of the unidirectional T800H/3631 laminate at a relatively high strain level is significantly influenced by the inelastic property of the epoxy resin employed. On the other hand, it was found that the nonlinear rate-dependent behavior of unidirectional PMC laminates subjected to off-axis loading is adequately described in terms of the

phenomenological viscoplasticity models[15)-17)] based on the overstress concept. In the present study, therefore, we attempted to evaluate the applicability of the rate form of a phenomenological viscoplasticity model for the observed off-axis stress relaxation behavior.

Applying a high stress or strain to polymers reactivates their physical aging[8)]. This suggests that the stress relaxation response of PMCs at relatively high strain levels should be treated as the so-called long-term behavior governed by complicated interactions between mechanical effects and physical aging of the polymer matrix employed. Presently, we have no sufficient data on the relevant time hardening/softening behavior of PMCs. Therefore, the material constants appearing in the viscoplasticity model were determined to fit the basic experimental data involving the effect of physical aging.

4.1 Modified Gates - Sun model

The phenomenological viscoplasticity models for the time- and rate-dependent behaviors of unidirectional composites were developed early on by Ha and Springer[13)] and Gates and Sun[15)]. Those models are characterized by the effective stress and effective strain.

The Gates - Sun model[15)] is based on the master relationship between the effective viscoplastic strain rate and effective overstress and is expressed as

$$\dot{\bar{\varepsilon}}^p=\left\langle\frac{\bar{H}}{K}\right\rangle^{1/m}, \tag{1}$$

where $\bar{H}$ is the effective overstress, and K and m are material constants. The angular brackets define the operation $\langle x\rangle=x\ (x\geq 0)$; $\langle x\rangle=0\ (x<0)$. The effective overstress $\bar{H}$ is a net stress that determines the magnitude of the viscoplastic strain rate and is defined as

$$\bar{H}=\bar{\sigma}-\bar{\sigma}^*, \tag{2}$$

where $\bar{\sigma}^*$ is called a quasi-static stress. Obviously, the viscoplastic strain rate vanishes when the applied effective stress agrees with the quasi-static stress.

For simple loading of coupon specimens, the effective stress and effective plastic strain can be expressed as[24)]

$$\bar{\sigma}=h(\theta)\sigma_x \tag{3}$$

$$\bar{\varepsilon}^p=\frac{1}{h(\theta)}\varepsilon_x^p, \tag{4}$$

where σ_x and ε_x^p stand for the applied axial stress and the resulting viscoplastic strain, respectively, and the orientation factor $h(\theta)$ is written in the form

$$h(\theta)=\sqrt{\frac{3}{2}(\sin^4\theta+2a_{66}\sin^2\theta\cos^2\theta)}. \tag{5}$$

The coefficient a_{66} is a parameter representing the anisotropy in the off-axis stress-strain relationship for the given unidirectional composite.

In the original Gates - Sun model[15)], the evolution equation of the effective quasi-static stress is written as

$$\bar{e}^p=A(\bar{\sigma}^*)^n, \tag{6}$$

where

$$\bar{e}^p=\frac{1}{h(\theta)}\left(\varepsilon_x-\frac{\sigma_x^*}{E_x}\right). \tag{7}$$

To evaluate the magnitude of the axial quasi-static stress σ_x^*, we must to solve the nonlinear algebraic equation.

The effective internal strain $\bar{e}^p$ given by Eq.(7) is not identical to the effective viscoplastic strain $\bar{\varepsilon}^p$, and the physical interpretation of $\bar{e}^p$ is not clear. In general internal variable theories, the evolution of the assumed internal variables is related to the development of overall viscoplastic strain in order to clarify the causality of the inelastic phenomena described. To remove the above-mentioned problem in the original Gates - Sun model, therefore, in the present study, we adopted a modified evolution equation of the quasi-static stress of the following form[16),17)]:

$$\dot{\bar{\sigma}}^*=B(\bar{\varepsilon}^p)^l\dot{\bar{\varepsilon}}^p. \tag{8}$$

The plane-stress viscoplasticity model using Eq.(8) instead of Eq.(6) is referred to as the modified Gates-Sun model hereafter.

4.2 Material identification

Five material constants K, m, a_{66}, B, and l are involved in the modified Gates - Sun model. Following the procedure developed in the Sun - Chen model[24)], we can identify the value of a_{66} in such a way that a single relationship between the effective stress and effective viscoplastic strain is obtained regardless of the fiber orientation. The axial viscoplastic strain was evaluated as

$$\varepsilon_x^p=\varepsilon_x-\frac{\sigma_x}{E_x}. \tag{9}$$

As a result of this procedure, the value of a_{66} came out as $a_{66}=1.3$. Figure 6 shows the single-curve approximation of the relationship between the effective stress and effective viscoplastic strain for the off-axis tension test results.

The axial quasi-static stress σ_x^* can be approximated as the stress level after five hours of relaxation, since the stress relaxation rate almost disappears in five hours, as observed in Figs. 4(a) - (c). Note that the quasi-static stress represents the stress level at which the viscoplastic strain rate vanishes. By fitting Eq.(8) to the experimental relationship between the effective quasi-static stress evaluated as above and the effective viscoplastic strain associated with the axial viscoplastic strain at the end of the stress relaxation, we obtained the following values:

$$B=70.88\ \text{MPa} \tag{10.a}$$

$$l=-0.67. \tag{10.b}$$

The remaining constants K and m in Eq.(1) can

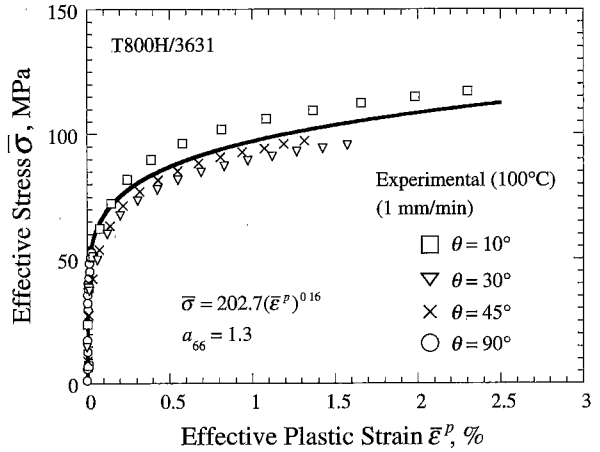

Fig. 6 Relationship between the effective stress and effective viscoplastic strain for unidirectional T800H/3631 at 100°C

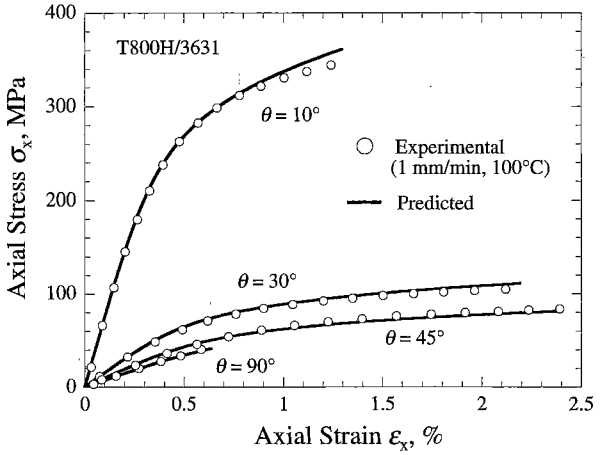

Fig. 7 Tensile stress-strain relationships predicted using the modified Gates-Sun model

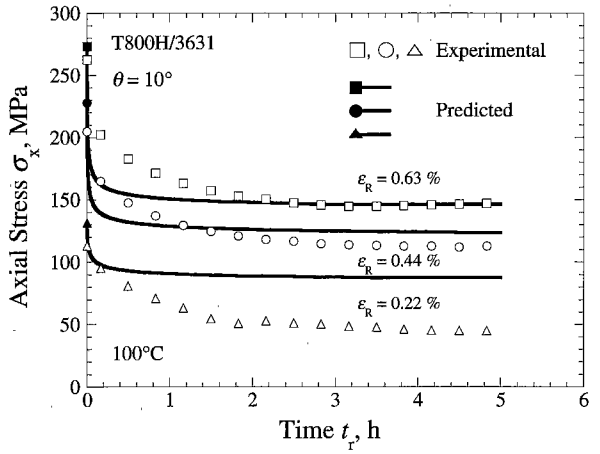

(a) θ=10°

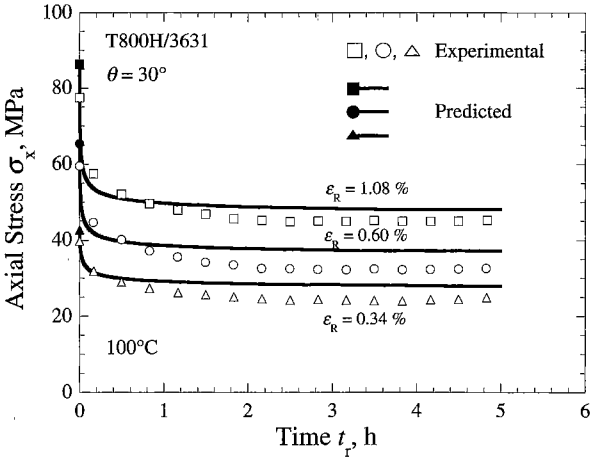

(b) θ=30°

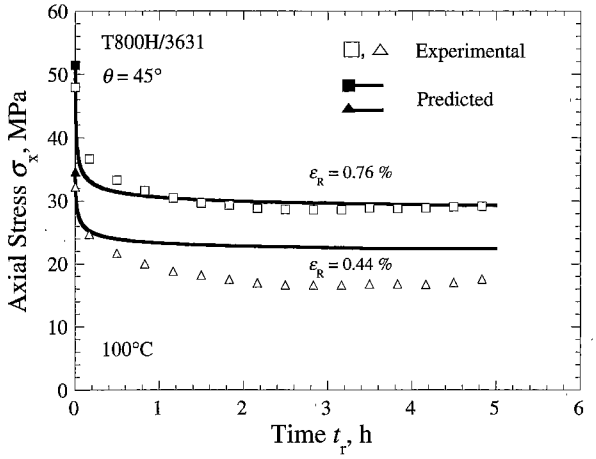

(c) θ=45°

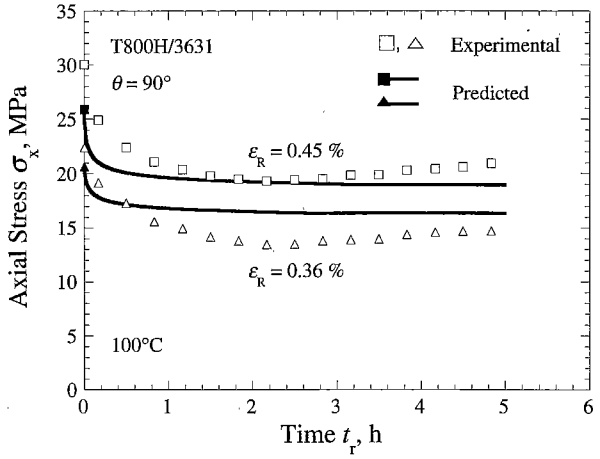

(d) θ=90°

Fig. 8 Off-axis stress relaxation responses predicted using the modified Gates-Sun model

be evaluated by a straight-line fit of the logarithmic plot of the master relationship between the effective overstress $\bar{H}$ and the effective viscoplastic strain rate $\dot{\bar{\varepsilon}}^p$. The values of K and m evaluated in this manner were slightly modified to reproduce the shapes of the off-axis stress-strain curves well and were

$K=162.5\ \mathrm{MPa}^m\mathrm{min}^m$ (11. a)

$m=0.275$. (11. b)

The off-axis stress - strain relationships predicted using the modified Gates - Sun model are compared with the experimental results in Fig. 7. We can confirm that good agreements are achieved.

4. 3 Off-axis stress relaxation simulation

Figures 8(a) - (d) show comparisons between the predicted and observed stress relaxation curves for $\theta=10$, 30, 45, and 90° respectively. Note that the entire process of the prior instantaneous response upon straining to a hold level and the subsequent stress relaxation behavior is simulated using the modified Gates - Sun model.

We note that the accuracy of predictions for the instantaneous behavior in Fig. 8 is not good as that in Fig. 7. More specifically, there is a discrepancy between the observed and predicted stress levels at the beginning of the relaxation responses shown in Figs. 8(a) - (d). This is because Figs. 7 and 8 show experimental results for different specimens; namely, the off-axis tensile response to instantaneous straining in Fig. 8 does not completely agree with that shown in Fig. 7. In view of the data scatter as well as the complex loading path simulated, we can conclude that the viscoplasticity model succeeds in satisfactorily describing the off-axis stress relaxation behavior of the unidirectional laminate.

To obtain better predictions of the off-axis stress relaxation behavior, we must improve the accuracy of the prediction of the stress relaxation rate just after the total strain is kept constant. The modified Gates - Sun model overestimates the stress relaxation rate at the beginning of the stress relaxation behavior; this feature is common to most viscoplasticity models based on the overstress concept. To control the magnitude of the initial rate of stress relaxation, we must refine the evolution equation for the quasi-static stress. Different kinds of variables may be necessary in a more precise description of the internal state of composite systems. In addition, a consideration of the loading condition in stress relaxation tests may also be required.

5. Conclusions

High-temperature off-axis stress relaxation behavior of the unidirectional T800H/3631 composite at relatively high strain levels was examined. The validity of a phenomenological viscoplasticity model for the description of the off-axis stress relaxation response was also evaluated by comparison with the experimental results. The results obtained can be summarized as follows.

(1) The stress relaxation effect is clearly observed for all fiber orientations ($\theta=10$, 30, 45, 90°). The amount of stress relaxation becomes more significant at a higher strain level.

(2) The stress relaxation rate quickly decreases just after the strain hold and it tends to vanish, regardless of the fiber orientation and the hold strain level.

(3) The stress relaxation modulus for a relatively high strain level depends on the strain kept constant, regardless of the fiber orientation. This result and the related evidence of permanent deformation upon loading imply that the stress relaxation behavior observed in this study is influenced by the time-dependent inelastic property of the polymer matrix employed.

(4) A modified form of the Gates - Sun phenomenological viscoplasticity model is adopted. The modified version is superior to the original form in its clear causality of the evolution of internal variable as well as easy numerical implementation.

(5) The modified Gates - Sun model satisfactorily reproduces the observed off-axis stress relaxation behavior for the unidirectional PMC system at 100°C.

(6) To improve the accuracy of predictions, we must consider a more precise description of the internal state of PMCs as well as the loading condition of the stress relaxation behavior observed.

References

(1) Vlack, L.H.V., Materials Science for Engineers, (1970), pp. 126-230, Addison-Wesley.

(2) Barrett, C.R., Nix, W.D. and Tetelman, A.S., The Principles of Engineering Materials, (1973), pp. 328-348, Prentice-Hall.

(3) Courtney, T.H., Mechanical Behavior of Materials, (1990), pp. 325-379, McGraw-Hill.

(4) Matsuoka, S., Relaxation Phenomena in Polymers, (1992), Carl Hanser Verlag.

(5) Nielsen, L.E., Mechanical Properties of Polymers and Composites, (1975), Marcel Dekker, New York.

(6) Beckwith, S.W., Creep Evaluation of a Glass/Epoxy Composite, SAMPE Quarterly, Vol. 11 (1980), pp. 8-15.

(7) Sullivan, J.L., Creep and Physical Aging of Composites, Composite Science and Technology, Vol. 39 (1990), pp. 207-232.

(8) Struik, L.C.E., Physical Aging in Amorphous Polymers and Other Materials, (1978), Elsevier, Amsterdam.

(9) Tuttle, M.E. and Brinson, H.F., Prediction of the Long-Term Creep Compliance of General Composites, Experimental Mechanics, Vol. 26, No. 1 (1986), pp. 89-102.

(10) Schapery, R.A., Viscoelastic Behavior and Analysis of Composite Materials, Mechanics of Composite Materials, (1974), pp. 85-168, Academic Press.

(11) Katouzian, M., Bruller, O.S. and Horoschenkoff,

A., On the Effect of Temperature on the Creep Behavior of Neat and Carbon Fiber Reinforced PEEK and Epoxy Resin, J. Composite Materials, Vol. 29, No. 3 (1995), pp. 372-387.

(12) Tuttle, M.E., Pasricha, A. and Emery, A.F., The Nonlinear Viscoelastic-Viscoplastic Behavior of IM7/5260 Composites, J. Composite Materials, Vol. 29, No. 15 (1995), pp. 2025-2046.

(13) Ha, S.K. and Springer, G.S., Time Dependent Behavior of Laminated Composite at Elevated Temperature, J. Composite Materials, Vol. 23 (1989), pp. 1159-1197.

(14) Perzyna, P., Fundamental Problems in Viscoplasticity, Advances in Applied Mechanics , edited by Kuerti, G., Vol. 9 (1966), pp. 243-377, Academic Press.

(15) Gates, T.S. and Sun, C.T., Elastic/Viscoplastic Constitutive Model for Fiber Reinforced Thermoplastic Composites, AIAA Journal, Vol. 29, No. 3 (1991), pp. 457-463.

(16) Wang, C., Sun, C.T. and Gates, T.S., Elastic/Viscoplastic Behavior of Fiber-Reinforced Thermoplastic Composites, J. of Reinforced Plastics and Composites, Vol. 15 (1996), pp. 360-377.

(17) Wang, C. and Sun, C.T., Experimental Characterization of Constitutive Models for PEEK Thermoplastic Composite at Heating Stage during Forming, J. Composite Materials, Vol. 31, No. 15 (1997), pp. 1480-1506.

(18) Chung, I., Sun, C.T. and Chang, I.Y., Modeling Creep in Thermoplastic Composites, J. Composite Materials, Vol. 27, No. 10 (1993), pp. 1009-1029.

(19) JIS K7073, Testing Method for Tensile Properties of Carbon Fiber-Reinforced Plastics, Japanese Industrial Standard, (1988), Japanese Standards Association.

(20) JIS K7087, Testing Method for Tension Creep of Carbon Fiber-Reinforced Plastics, Japanese Industrial Standard, (1996), Japanese Standards Association.

(21) Kawai, M., Off-Axis Creep Behavior of Unidirectional Polymer Matrix Composites at High Temperature, IUTAM Symposium on Creep in Structures, (2001), pp. 469-478, Kluwer Academic Publishers.

(22) Gibson, R.F., Principles of Composite Material Mechanics, (1994), McGraw-Hill.

(23) Hull, D. and Clyne, T.W., An Introduction to Composite Materials, 2nd edition, (1996), Cambridge.

(24) Sun, C.T. and Chen, J.L., A Simple Flow Rule for Characterizing Nonlinear Behavior of Fiber Composites, J. Composite Materials, Vol. 23 (1989), pp. 1009-1020.